Oxygen intercalation in the perovskite superconductor $YBa_2Cu_3O_{6+x}$

W. R. McKinnon, M. L. Post, L. S. Selwyn, and G. Pleizier
Solid State Chemistry Section, Division of Chemistry, National Research Council of Canada, Ottawa, Canada K1A 0R9

J. M. Tarascon, P. Barboux, L. H. Greene, and G. W. Hull
Bell Communications Research, 331 Newman Springs Road, Red Bank, New Jersey 07701
(Received 30 November 1987; revised manuscript received 20 June 1988)

We have studied superconductivity and the thermodynamics of oxygen insertion in the oxygen intercalation system $YBa_2Cu_3O_{6+x}$. The superconducting transition temperature decreases as x decreases, and the transition is sharp at $T_c = 90$ K near $x = 1$ and at 55 K near $x = 0.5$. The thermodynamics of oxygen intercalation at high temperatures (both isotherms and isobars), and the orthorhombic-tetragonal transition, can be explained in terms of a lattice-gas model that includes a large energy of repulsion between oxygen atoms on nearest-neighbor sites. The high-temperature behavior is also consistent with smaller interactions, some attractive, between second neighbors. Such energies are needed to explain the behavior at low temperatures.

I. INTRODUCTION

The superconductor $YBa_2Cu_3O_{7-y}$ and the isostructural compounds with Y replaced by rare-earth ions are perovskites with ordered oxygen vacancies. All the oxygen is missing from the Y plane,[1] and half of the oxygen is missing from the Cu-O plane located between Ba-O planes.[2] The oxygen in this Cu-O plane occupies sites between Cu atoms along the crystallographic direction b but not along a, and the structure is orthorhombic. When $YBa_2Cu_3O_{7-y}$ is heated under vacuum, oxygen leaves the sites; at low oxygen content (x near 0 in $YBa_2Cu_3O_{6+x}$ or y near 1 in $YBa_2Cu_3O_{7-y}$), the remaining oxygen occupies sites both along a and along b, and the structure is tetragonal.[3] At low x, this tetragonal phase is not superconducting.[4]

At high temperatures (above about 700 K) the transition between these two structures is apparently continuous as the oxygen content varies with temperature and oxygen partial pressure, and occurs near $x = 0.6$.[5] This order-disorder transition can be understood at least qualitatively with a simple lattice-gas model that treats repulsions between nearest-neighbor oxygen atoms on a square lattice of sites.[6,7] In this model, atoms of oxygen are lost from each chain in the structure until the chains collapse at some critical value of x. But the behavior at lower temperatures is more complicated. Samples inhomogeneous in oxygen show two superconducting transitions, near 90 and 60 K,[8] and a plot of the superconducting transition temperature T_c as a function of oxygen content in more homogeneous samples has plateaus at these two temperatures.[9] Moreover, electron diffraction shows that near $x = 0.6$ the unit cell doubles along the crystallographic a direction,[10] suggesting that at room temperature at this x oxygen is missing from every other chain, rather than from all the chains. This additional ordering can be explained by lattice-gas models that include anisotropic second-neighbor interactions.[11]

To explore how well lattice-gas models describe the oxygen intercalation in $YBa_2Cu_3O_{6+x}$, we measured the thermodynamics of oxygen absorption in $YBa_2Cu_3O_{6+x}$ for $0 < x < 1$, both at constant pressure (isobars) using thermogravimetric analysis (TGA), and at constant temperatures (isotherms) at 923 K. We compare these results with the behavior expected from lattice-gas models, using expressions for the chemical potential that hold in some limiting cases, and using Monte Carlo techniques to calculate the chemical potential for explicit values of the interactions between oxygen atoms. These calculations show that the simplest model consistent with the order-disorder transition at high temperature describes the data, but with some discrepancies at higher x. By comparing the experimental results with calculations that include the longer-range interactions needed to explain the low-temperature structures, we set limits on the size of these interactions.

We also prepared two series of samples of different oxygen contents, either by adding oxygen to a sample with x near 0 and cooling in a nearly fixed oxygen pressure, or by heating a sample with x near 1 in argon. These samples are made in the same equipment where the thermodynamics were measured, and so even though the absolute errors on oxygen content are about 0.1, the errors on differences in x between these samples and the data obtained at high temperature is about 10 times smaller. We report the lattice parameters and Meissner effect in these samples. At room temperature, the orthorhombic structure is present over the range $0.3 < x < 1$, a wider range than at 1000 K, and the superconducting transition is sharp at 55 K for $0.5 < x < 0.6$. We argue that the increase of the range of the orthorhombic phase and the sharp transition at 55 K are caused by the longer-range interactions in the lattice-gas model. These interactions could produce complicated phase diagrams at low temperatures, similar to those found for staging in graphite.[12]

Section II describes the experimental procedure used to prepare the samples and measure the thermodynamics, and discusses the errors in oxygen content. Section III

presents the results. Section IV discusses what information can be derived with a comparison of the two thermodynamic measurements, based on general behavior of lattice-gas models, and Sec. V compares the numeric calculations with the experimental data. Section VI presents our conclusions.

II. EXPERIMENTAL PROCEDURE

The compound $YBa_2Cu_3O_{6+x}$ with x near 1 was prepared as described in Ref. 4. The x-ray diffraction pattern showed small unidentified Bragg peaks, indicating the sample was contaminated with up to a few percent of a crystalline phase.

Isobars were measured in a commercial TGA unit. Samples of 20 mg were heated or cooled at 4 K/min in a flow of argon and oxygen at a total pressure of 0.1 MPa. Relative values of x were determined to an accuracy of 1%. The ratio $[Ar/O_2]$ in the flow was monitored to within 2%.

Isotherms were measured using standard pressure-composition-temperature (p-c-T) techniques,[13] with samples of mass 8 g in an stainless-steel reactor of volume 7 cm^3, attached to a stainless-steel manifold (volume 29 cm^3). The manifold was equipped with oxygen and vacuum sources, and the oxygen content was changed by gas titration between the manifold and the reactor. The change in oxygen content was calculated from the oxygen pressure p and volumes of the system. For 0 MPa $< p <$ 0.2 MPa, pressure differences were measured to ± 7 Pa; at higher pressures, the errors were ± 30 Pa. Changes in oxygen content were measured to $\pm 0.002 \times 10^{-3}$ mole O_2. Other uncertainties such as the accuracy of the pressure transducers (0.1%) and errors in volume calibration (0.5%) increase the estimated errors in x to $\pm 1\%$.

We made identical measurements on the empty manifold, and found that it appeared to absorb oxygen above 0.1 MPa. This apparent absorption could be due to a reaction with the chamber walls or due to errors in our calculation of gas volumes. [The effective volume of the sample chamber is determined by the temperature profile between the sample chamber (typically at 923 K) and the manifold (at room temperature). This temperature profile can change as the gas pressure changes.] The apparent composition in the empty chamber increased roughly linearly with pressure, and we used a linear fit to correct our data. The corrections to increments in x with changes in gas pressure are 5% at 0.1 MPa and larger than 30% at 0.5 MPa. We do not consider the corrections above 0.5 MPa to be reliable, and so only report the results to 0.5 MPa.

We measured several isotherms on the same sample, and started each one from a reference state, which was obtained by heating the sample at 923 K overnight under a vacuum of 0.01 Pa. As a check that most of the oxygen had been removed, we isolated the sample and manifold from the vacuum, and heated them to 1023 K. The amount of gas evolved corresponded to a change in x of less than 0.001. We also measured the isotherms on desorption (decreasing x) and found results indistinguishable from those obtained on absorption (increasing x).

A series of compounds of varying oxygen content was prepared in the TGA apparatus. All the compounds were made from the same starting material, which we took to be $YBa_2Cu_3O_7$. Compounds were heated in argon at 1 K/min until a specified weight was lost, then cooled as fast as possible (about 100 K/min). Both powders and bars were prepared in this way. The Hall effect of the bars has been reported elsewhere.[14]

A second series was prepared in the p-c-T apparatus. A sample of about 6 g was prepared in the reference state described above. Aliquots of oxygen were added to this sample in the following way. The oxygen pressure was adjusted to some value, the sample was equilibrated for one hour at 923 K, and then cooled over several hours to room temperature. Over 98% of the oxygen was absorbed above 700 K. The composition of the sample at room temperature was calculated from the amount of oxygen absorbed. About 200 mg of the sample was removed, and the remaining sample was reattached to the manifold, the chamber flushed with oxygen, the previous oxygen pressure reestablished, and the sample reheated to 923 K. The procedure was repeated at an increased oxygen pressure. The errors in composition accumulate throughout this procedure, and we estimate an error of ± 0.03 for $x < 0.5$, increasing to ± 0.08 for the final sample. The stainless-steel container contaminated the samples with traces of Fe, Cr, and Ni, to a total level of 0.2% by weight, as determined by dc arc spectrography. Since the samples with the largest x were made last, they spent the longest time in the sample chamber and so are the most contaminated.

The lattice parameters of both series of samples were determined by least-squares refinement of about 25 peaks in powder x-ray diffraction. We measured the powder patterns of the same slides of the second set of samples after two months, and found that samples with low x had decomposed into Y_2BaCuO_5, $BaCO_3$, and other compounds. The degree of decomposition was inversely related to x; the sample with the lowest x had almost completely decomposed, whereas that with the largest x showed no decomposition.

The dc magnetic susceptibility was measured with a SQUID (superconducting quantum interference device) magnetometer. The ac magnetic susceptibility was measured with a mutual-inductance technique at 13 Hz.

III. RESULTS

The absolute oxygen content in $YBa_2Cu_3O_{6+x}$ of these samples has been determined only to about ± 0.1.[4] Samples cooled slowly in oxygen are close to $YBa_2Cu_3O_7$, and those annealed under vacuum are close to $YBa_2Cu_3O_6$. Since we start from oxygen-annealed samples in the TGA apparatus and vacuum-annealed ones in the p-c-T apparatus, we have to assign compositions to these two end points to connect the two sets of samples. We have chosen to assign $x = 1$ to those samples slowly cooled in one atmosphere of oxygen. With this assignment, the lowest value of x reached in the TGA samples was $x = 0.09$. We thus

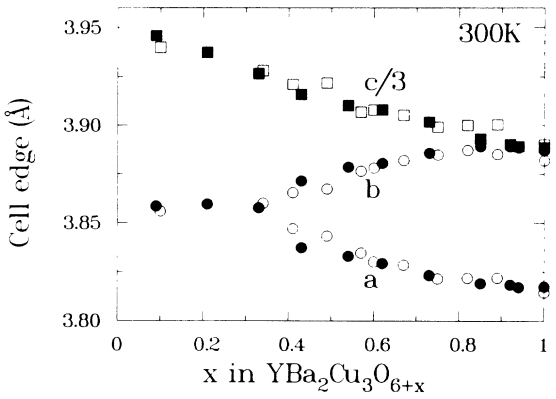

FIG. 1. Edges of the orthorhombic or tetragonal unit cells in $YBa_2Cu_3O_{6+x}$ vs x at 300 K for the two sets of samples described in the text. Open symbols: prepared by heating in argon. Closed symbols: prepared by cooling in oxygen.

expect this to be the composition of the starting material in the *p-c-T* apparatus, and so we have taken our reference sample (annealed in 923 K in vacuum) to have $x=0.09$. Although absolute values of x may be in error by ± 0.1, relative values are probably correct to ± 0.01.

A. Room temperature and below

Figure 1 shows the lattice parameters vs x for the two series of samples prepared as described above. The data are also reported in Tables I and II. In both series, for the highest value of x indexed as tetragonal ($x=0.34$ and $x=0.33$), the Bragg peaks that split in the orthorhombic phase were broader than at lower x, suggesting a small orthorhombic distortion; thus the phase boundary between the tetragonal and orthorhombic phase is near $x=0.3$. Figure 2 shows the Meissner effect as a function of temperature in the two sets of samples. In both series of samples, the superconducting transitions are sharp near 90 K for x near 1. As x decreases, the transition shifts to lower temperature and broadens, sharpening near 55 K for x between 0.5 and 0.6. Both series show no superconductivity below $x=0.2$. The sharp transitions at 90 and 55 K are consistent with the measurement of two transitions, one

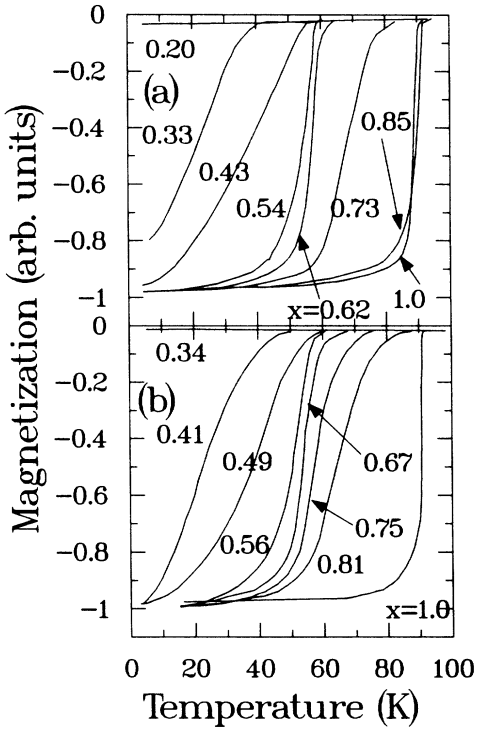

FIG. 2. dc magnetization vs x in $YBa_2Cu_3O_{6+x}$ for the two sets of samples described in the text, for cooling in a field of 100 Oe. (a) Samples prepared by cooling in oxygen; (b) samples prepared by heating in argon.

TABLE I. Samples of $YBa_2Cu_3O_{6+x}$ prepared by heating $YBa_2Cu_3O_7$ in argon. a, b, and c are the edges of the orthorhombic or tetragonal unit cells. T_{onset}^{dc} and T_{sat}^{dc} are the temperatures at which diamagnetism begins and at which it saturates, for the dc magnetization determined on warming the sample. These temperatures were determined by drawing the tangent to the maximum slope of the magnetization curve, and finding its intercepts with zero magnetism and with the maximum magnetization attained at low temperature. The percent of superconductivity was determined from the flux expelled during cooling, taking the mass of the sample and the crystallography density of the compound.

x	a (Å)	b (Å)	c (Å)	T_{onset}^{dc} (K)	T_{sat}^{dc} (K)	% Meissner (%)
1.00	3.815(1)	3.882(1)	11.67(2)	90	87	35
0.89	3.822(1)	3.885(1)	11.70(1)	76	51	28
0.82	3.822(1)	3.887(1)	11.70(2)	84	60	23
0.75	3.822(1)	3.885(1)	11.70(2)	65	50	30
0.67	3.829(1)	3.882(1)	11.72(2)	60	48	27
0.60	3.830(1)	3.878(1)	11.72(1)	. . .	. . .	. . .
0.57	3.835(1)	3.876(1)	11.72(2)	58	42	27
0.49	3.843(1)	3.867(1)	11.77(2)	52	19	21
0.41	3.847(1)	3.865(1)	11.76(3)	40	10	11
0.34	3.860(1)	3.860(1)	11.78(5)	0	0	0
0.10	3.856(1)	3.856(1)	11.82(3)	0	0	0

TABLE II. Samples of $YBa_2Cu_3O_{6+x}$ prepared by cooling $YBa_2Cu_3O_6$ in oxygen. As in Table I, except the onset and saturation of diagmagnetism are from the ac magnetization.

x	a (Å)	b (Å)	c (Å)	T_{onset}^{ac} (K)	T_{sat}^{ac} (K)	% Meissner (%)
1.00	3.818(1)	3.887(1)	11.67(2)	86	80	28
0.94	3.817(1)	3.888(1)	11.67(2)	86	83	28
0.92	3.819(1)	3.889(1)	11.67(2)	93	86	29
0.85	3.819(1)	3.889(1)	11.68(3)	93	86	21
0.73	3.823(1)	3.886(1)	11.71(3)	86	59	19
0.62	3.829(1)	3.880(1)	11.72(3)	61	50	26
0.54	3.833(1)	3.879(1)	11.73(3)	60	50	25
0.43	3.837(1)	3.871(1)	11.75(3)	59	31	17
0.33	3.858(2)	3.858(2)	11.78(8)	41	27	7
0.21	3.859(1)	3.859(1)	11.81(7)	0	0	0
0.09	3.858(1)	3.858(1)	11.84(6)	0	0	0

near 90 K and the other near 55 K, in inhomogeneous samples.[8]

In the samples with the largest x prepared in the p-c-T apparatus, T_c is 1–2 K lower than the maximum value seen at lower x. These samples were taken to higher pressures than any of the samples prepared in the TGA apparatus. Although the x-ray powder patterns showed no evidence of decomposition, we and others[15] have seen the samples decompose at higher pressures. Thus the reduction in T_c might be due to such decomposition. It could also be related to the contamination of the samples by iron from the sample container, since iron reduces T_c in these systems.[16]

B. Thermodynamics at higher temperatures

Figure 3 shows a series of isobars measured as the samples were cooled at 4 K/min. The kinks in the curves, indicated by the solid circle, are associated with the order-disorder transition of oxygen,[15] as expected from the lattice-gas model presented in Ref. 6 and that discussed below. In each case the curves were shifted so that they reached $x=1$ at the lowest temperature (473 or 523 K). With this shift, the order-disorder transition as defined by the kink occurs at $x=0.6$. Jorgensen *et al.*[5] have refined the oxygen content at the order-disorder transition near 900 K to be $x=0.5$. These two values are within the combined uncertainties in the two determinations.

Figure 4 shows the isotherm at 923 K. The chemical potential of oxygen atoms is calculated from the pressure for an ideal-gas law for oxygen:

$$\mu = \frac{k_B T}{2} \ln\left(\frac{p}{aT^{5/2}}\right), \tag{1}$$

where $a=0.4635$ for oxygen with p in MPa and T in K.

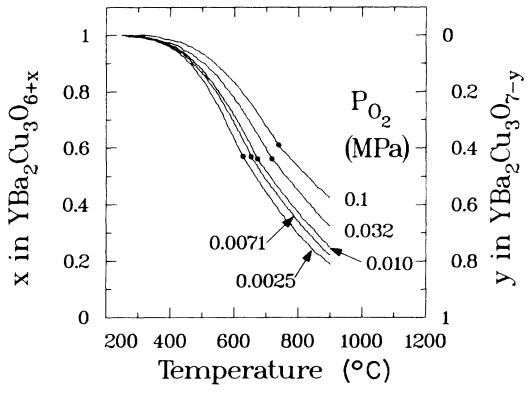

FIG. 3. Isotherms for $YBa_2Cu_3O_{6+x}$, obtained on cooling a sample of 4 K/min in a mixture of oxygen and argon at a total pressure of 0.1 MPa. The partial pressures of oxygen in MPa are indicated. The solid circles are our estimate of where the change in slope occurs, signaling the order-disorder transition discussed in the text.

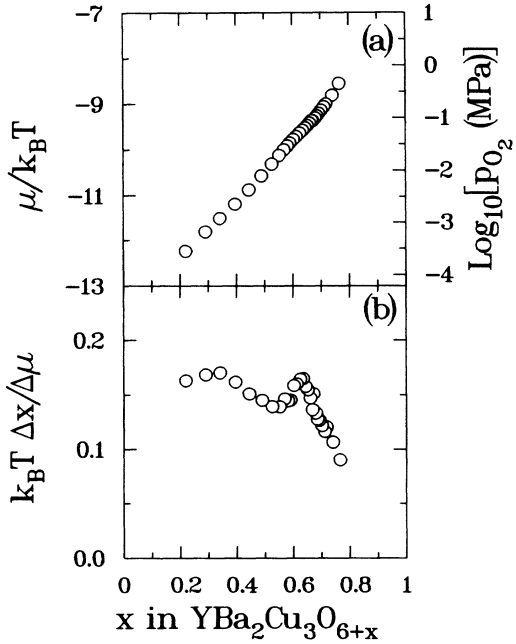

FIG. 4. (a) Isobar for $YBa_2Cu_3O_{6+x}$ measured at 923 K. The pressure in MPa is converted to the chemical potential μ using Eq. (1) in the text. (b) The derivative $(\partial x/\partial\mu)_T$ calculated from (a).

(The ideal-gas law accurately describes the thermodynamics of oxygen gas under the conditions used, as a comparison of experiment and theory shows.[17]) We could measure the isotherms accurately over only a partial range of x at any temperature. As temperature increases the isotherms move to higher pressure, and we cannot reach the pressures needed to fill the lattice to $x=1$ in $YBa_2Cu_3O_{6+x}$. At lower temperatures, the kinetics of intercalation slows over the entire range of x, and the pressure at low x becomes too small to measure accurately. Within the scatter of the data, the isotherm and its derivative were identical when remeasured at 923 K, or measured at 903 K.

The curve in Fig. 4 shows a kink, which appears as a peak or step in the inverse derivative. We plot $(\partial x/\partial u)_T$ because, as in other intercalation systems,[18] this quantity is a thermodynamic response function analogous to specific heat or compressibility. In particular, $(\partial x/\partial \mu)_T$ has peaks at phase transitions. The peak in Fig. 4 near $x=0.6$ corresponds to the kink in the isobars in Fig. 3 at $x=0.6$, and indicates the transition between the orthorhombic and tetragonal structures. The difference between the composition of the order-disorder transition at 923 K and that seen in samples at room temperature in Fig. 1 is about 0.3, and the error in this difference should be considerably smaller than the possible error of 0.1 in absolute values of x, because both these values of x are determined in the same apparatus.

Whereas peaks in $(\partial x/\partial \mu)_T$ are produced by the fluctuations associated with phase transitions, minima in $(\partial x/\partial \mu)_T$ are associated with stability, and occur at the compositions of ordered structures, even if there is only short-range order present.[19,20] Thus the minimum at $x=0.5$ may indicate short-range order at this composition, although it could simply be caused by the peak in $(\partial x/\partial \mu)_T$ sitting on the side of a broad maximum.

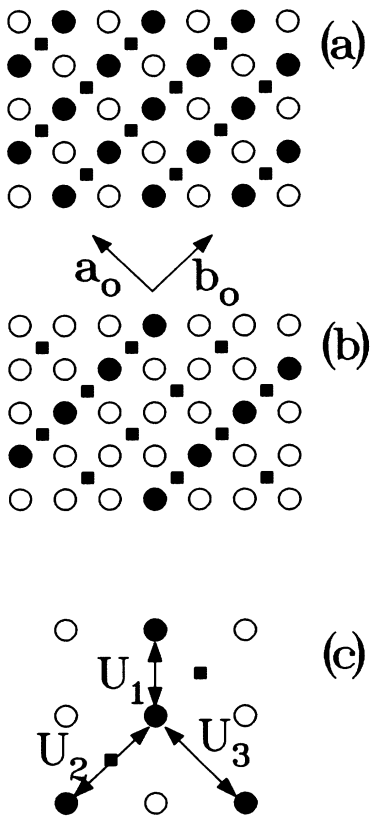

FIG. 5. Lattice for oxygen intercalation in the Cu-O planes between Ba-O planes in $YBa_2Cu_3O_{6+x}$. Solid squares are Cu, open circles are empty oxygen sites, and filled circles are filled oxygen sites. (a) Ordered structure at $x=1$. (b) Ordered structure near $x=0.5$. (c) Energies of interaction between oxygen atoms on nearest-neighbor and next-nearest-neighbor sites.

IV. COMPARISON OF ISOTHERMS AND ISOBARS

Before turning to calculations of lattice-gas models, we consider whether a comparison of the isotherms and isobars can suggest the magnitudes of some of the interactions of such models. Figure 5(a) shows the Cu-O plane between planes of Ba-O near $x=1$. For this ordered state there are no nearest-neighbor oxygen pairs. That it is impossible to go beyond $x=1$ suggests the nearest-neighbor repulsion is large enough to forbid any nearest-neighbor interactions. In this case, the actual magnitude of the nearest-neighbor interaction drops out of the expression for the chemical potential; in effect, the large nearest-neighbor repulsion is replaced by a rule that states: never place two oxygen atoms on adjacent sites. Thus this interaction modifies the configurational entropy of distributing the atoms through the lattice, but otherwise does not enter the expression for chemical potential. If this were the only interaction between oxygen atoms in the lattice, the chemical potential would take the following form:

$$\mu=\varepsilon_O-Ts_O+k_BTf(x)\,. \tag{2}$$

Here ε_O and s_O denote the energy and entropy parts of the chemical potential from an isolated oxygen (the "site" values), and the third term, involving $f(x)$, a function of x alone, arises from the entropy of distributing the atoms over the sites in the lattice subject to the constraint that there be no nearest neighbors.

If Eq. (2) holds, then the derivative $(\partial x/\partial \mu)_T$ at some fixed temperature T_0 should be related to the temperature derivative of the TGA results, $T(\partial x/\partial T)_p$, as follows. Rewriting Eq. (2) as

$$f(x)=\frac{\mu}{k_BT}-\frac{\varepsilon_O}{k_BT}+\frac{s_O}{k_B}\,, \tag{3}$$

and differentiating with respect to either μ or T gives

$$\begin{aligned}\frac{df}{dx}\left(\frac{\partial x}{\partial \mu}\right)_{T=T_0}&=\frac{1}{k_BT_0}\,,\\ \frac{df}{dx}\left(\frac{\partial x}{\partial T}\right)_p&=\frac{\varepsilon_O}{k_BT^2}-\frac{5}{4T}\,.\end{aligned} \tag{4}$$

In the differentiation at constant p, μ has been replaced by the right-hand side of Eq. (1). Eliminating df/dx in Eq.

(4) gives

$$\left[k_B T_0 \frac{\partial x}{\partial \mu}\right]_{T=T_0} = \frac{1}{\varepsilon_0/k_B T - \frac{5}{4}} T \left[\frac{\partial x}{\partial T}\right]_p . \quad (5)$$

Figure 6(a) compares $(\partial x/\partial \mu)_T$ from Fig. 4 with the value calculated with Eq. (5) from one of the curves in Fig. 3. The comparison suggests that Eq. (2) is a reasonable starting point, especially since the other TGA curves in Fig. 3 give the same curve for $(\partial x/\partial \mu)_T$ within the scatter of the data. The value of $\varepsilon_0 = -0.9$ eV used in the comparison is within 10% of the heat of solution of oxygen measured in Ref. 21.

There is a difference between the two curves in Fig. 6, and this difference could be consistent with additional interactions. If these interactions are comparable to $k_B T$, they will modify the configurational entropy term $f(x)$ in Eq. (2) and introduce an additional energy term. To treat this requires model calculations like those described below. But as a first approximation we can consider a mean-field treatment. Suppose the additional interactions are weak or of long range, so they do not modify $f(x)$, but only introduce a term $U_0 x$ into Eq. (2), giving

$$\mu = \varepsilon_0 - T s_0 + k_B T f(x) + U_0 x . \quad (6)$$

Then an analysis like that used to derive Eq. (5) shows that $T(\partial x/\partial T)_p$ can be used to calculate $(\partial x/\partial \mu)_T$ at a temperature T_0 according to the following equation:

$$\left[k_B T_0 \left[\frac{\partial x}{\partial \mu}\right]_{T=T_0}\right]^{-1} = \left[\frac{\varepsilon_0 + U_0 x}{k_B T} - \frac{5}{4}\right]\left[T\left[\frac{\partial x}{\partial T}\right]_p\right]^{-1} + \frac{U_0}{k_B}\left[\frac{1}{T_0} - \frac{1}{T}\right] . \quad (7)$$

Adjusting the two parameters ε_0 and U_0 in Eq. (7) improves the agreement between the measured $(\partial x/\partial \mu)_T$ and that calculated from $T(\partial x/\partial T)_p$, as Fig. 6(b) shows. The value $U_0 = -4 k_B T_0$ that gives the best agreement is large, and so unless the interactions are long range Eq. (6) is not valid. Moreover, there are systematic errors of several degrees in the temperatures of the isobars in Fig. 3, so these data are less accurate than the isotherm in Fig. 4. Nevertheless, we see that the isobars and isotherms, while consistent with a large nearest-neighbor interaction, also allow other interactions.

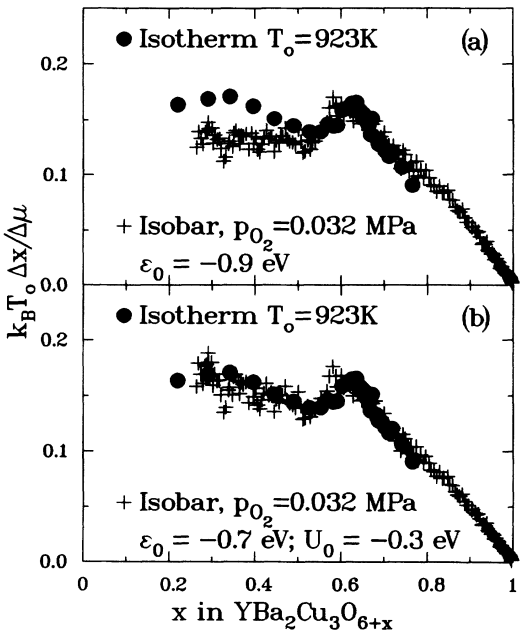

FIG. 6. Comparison of $(\partial x/\partial \mu)_T$ measured from the isotherm in Fig. 4 and that calculated from the isobar at $p = 0.032$ MPa from Fig. 3 using (a) Eq. (5) and (b) Eq. (7). From Eq. (5), the site energy is $\varepsilon_0 = -0.9$ eV, and from Eq. (7), $\varepsilon_0 = -0.7$ eV and $U_0 = -0.3$ eV.

V. LATTICE-GAS MODELS

A. Nearest-neighbor interactions

As discussed in Sec. IV, the lattice of sites available for oxygen is a simple square lattice, and the structure at $x = 1$ can be viewed as an ordering of the oxygen in which nearest-neighbor sites are never simultaneously occupied. This exclusion of nearest neighbors implies that oxygen ions strongly repel ions on adjacent sites. Such a repulsion, of energy U_1, might be a direct Coulomb repulsion between the negative oxygen ions. More likely, it is associated with the stability of the square coordination of Cu by O. A Cu atom between two diagonally opposite oxygens, with the other two oxygen sites next to the Cu empty, has square-planar coordination, since there are also oxygens above and below it. Adding a third oxygen, and forming nearest-neighbor oxygen pairs, destroys the square-planar coordination, and costs energy compared to adding that oxygen elsewhere. That energy determines U_1.

Figure 7 shows the phase diagram for the lattice-gas model on a square lattice, with nearest-neighbor repulsive interactions only, as a plot of temperature (in units of U_1/k_B) versus the fraction of sites filled. For our

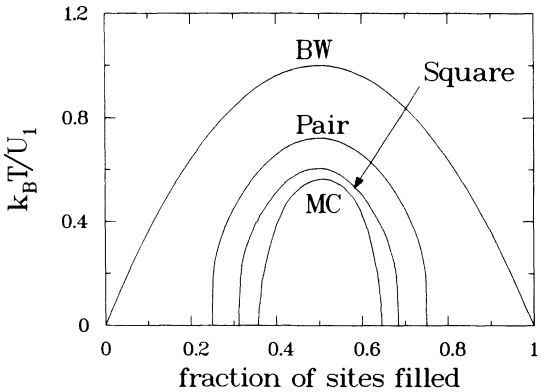

FIG. 7. Phase diagrams for the lattice-gas model on a square lattice, with nearest-neighbor interactions U_1 and second-neighbor interactions U_2. BW, Bragg-Williams; Pair, pair or quasichemical approximation of the cluster variation method (Ref. 23); Square, square approximation of the cluster variation method (Ref. 7); MC, Monte Carlo calculation (Ref. 22).

definition of x in $YBa_2Cu_3O_{6+x}$ the fraction of filled sites in Fig. 7 corresponds to $x/2$, and the right half of the phase diagram, corresponding to filling more than half of the sites, is not accessible experimentally. The phase diagram calculated by Binder and Landau[22] using Monte Carlo (MC) calculations is compared to that calculated in the Bragg-Williams (BW) approximation and the pair[23] approximations of the cluster variation method (CVM). All these approximations are qualitatively correct: each gives a disordered phase (corresponding to the tetragonal form of $YBa_2Cu_3O_{6+x}$) at all x at high temperatures, and at small and large x for all temperatures; and each gives an ordered phase (corresponding to orthorhombic $YBa_2Cu_3O_{6+x}$) at low temperatures and intermediate x. But for quantitative comparison of calculation and experiment, it is essential to use a calculation as good as a MC or a higher-order CVM calculation. Bakker, Welch, and Lazareth[6] discuss the order-disorder transition in $YBa_2Cu_3O_{6+x}$ using the pair approximations of the CVM, and claim good agreement with the calculated composition of the order-disorder transition (near $x=0.5$) and that measured in Ref. 5. But that agreement is fortuitous, a result of the approximation used. According to the Monte Carlo calculations[22] (which agree with other estimates) the order-disorder transition occurs at $x=0.71$.

As discussed above, μ does not depend on the strength of a short-range repulsive interaction once that interaction becomes large. Thus the calculation of μ is independent of U_1 for U_1 above $5k_BT$. Figure 8 compares the experimental isotherm at 923 K with that calculated by Monte Carlo and the square approximation of the cluster variation method. The Monte Carlo calculations were performed using the methods in Ref. 24, for a 32×32 square lattice; for each value of μ, 200 passes over the lattice were made to thermalize the lattice, and then 2000 passes were made to calculate averages. $(\partial x/\partial\mu)_T$ was calculated from the fluctuations in x. The CVM equations in the square approximation were iterated as described in Ref. 25. The only parameter adjusted for comparing calculated values of μ with experiment was the value of $\mu_0=\varepsilon_O-T_0s_O$, set to $-10.8k_BT_0=-0.86$ eV in Fig. 8(a), and there are no adjustable parameters in Fig. 8(b). The agreement at low x, and the peak in $(\partial x/\partial\mu)_T$ at approximately the right composition (but calculated to be about 0.1 too large in x) suggests this model is essentially correct. The largest discrepancy is at large x, where the calculated μ varies too slowly with x, or, equivalently, where the calculated $(\partial x/\partial\mu)_T$ is too large. We have explored various other interactions (see below), and can find no convincing way to reduce this discrepancy without losing the agreement at lower x. It is conceivable that there is an effect on μ from the changing electronic state of Cu, if holes are added to a Cu d band as x increases. But treating this effect requires separating μ into ionic and electronic contributions. This separation has been studied in other intercalation systems, where it is found that the screening between ions and electrons is an essential part of the problem.[26,27] Since the electronic structure of these materials is still being debated, we do not know how to treat this screening here.

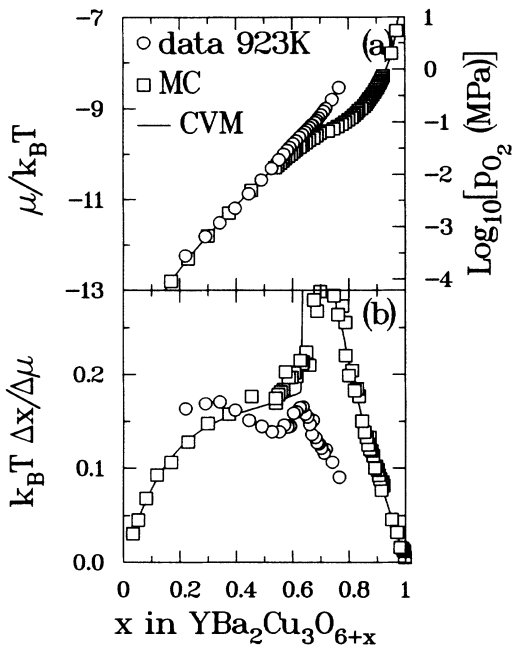

FIG. 8. Comparison of calculation and experiment for (a) μ and (b) $(\partial x/\partial\mu)_T$ at 923 K. Solid circles are data from Fig. 4. Open squares are MC calculations and solid line is a CVM calculation, for nearest-neighbor interactions U_1 only. The calculations are independent of U_1 for U_1 larger than $5k_BT$; the calculations shown are for $U_1=16k_BT/3$.

We do not expect there to be much difference between the calculations in Fig. 8, based on a two-dimensional lattice, and those that would be obtained from a three-dimensional lattice-gas model that considers weak interactions between oxygen atoms in different layers in the $YBa_2Cu_3O_{6+x}$ structure. Such three-dimensional effects would be strongest in the critical region near the order-disorder phase transition. The width of this region should correspond roughly to the region near the peak in $(\partial x/\partial\mu)_T$ where the MC and CVM calculations disagree,[20] because there the fluctuations extend over long distances. The agreement between CVM, which treats the fluctuations only over a square of oxygen sites, and the MC calculations, which considers a finite lattice 32 sites on a side, suggest fluctuations over long distances are unimportant except for a region of about $\Delta x=0.1$ near $x=0.7$. Thus small interactions normal to the layers will probably modify the calculated values of $(\partial x/\partial\mu)_T$ only over this region.

B. Second-neighbor interactions

Adding second-neighbor interactions to the problem does not improve the agreement with experiment, but because these interactions are needed to explain the low-temperature behavior, we explored their effects on μ. Since we believe the calculation in Fig. 8 is the best that can be done with this lattice-gas model, we suggest that other interactions must be smaller than those values which significantly worsen the agreement with experiment.

The ordered state observed near $x=0.5$ doubles the unit cell in the orthorhombic a direction,[10,28] suggesting that it

corresponds to alternating full and empty chains, as shown in Fig. 5(b). Such an ordered state can be generated in a lattice-gas model that considers the anisotropy in the second-neighbor interaction.[11] The interactions considered are shown in Fig. 5(c). If the interaction between oxygen atoms is attractive for oxygens separated by a copper atom (U_2 negative), the oxygens will cluster into chains; if the interaction is repulsive between second-neighbor oxygens not separated by Cu (U_3 positive), full chains will repel one another, leading to an ordered state of alternating full and empty states. Thus we considered these interactions in the Monte Carlo calculations.

Figure 9 compares experiment with calculation for several values of these interactions. For small U_2 and U_3, these interactions do not modify the configurational entropy, and so they can be considered in mean-field theory, as in Eq. (6):

$$\mu = \varepsilon_O - Ts_O + k_B T f(x) + (U_2 + U_3)x . \quad (8)$$

If U_2 and U_3 are equal and opposite, they cancel in Eq. (8), and so will not affect μ until they become large enough to affect $f(x)$. Figure 9 shows that they barely have an effect at $U_3 = -U_2 = k_B T$. At twice this value, however, a minimum appears in $(\partial x/\partial \mu)_T$ at $x = 0.5$, caused by short-range order at this composition. This minimum depends more on the repulsive U_3 than on the attractive U_2, as seen by reducing U_3 and leaving U_2 unchanged. In fact, for $U_2 = -2k_B T$ and $U_3 = k_B T$, the peak in $(\partial x/\partial \mu)_T$ moves to lower x, closer to the experimental value, but at the expense of increasing $(\partial x/\partial \mu)_T$ and so worsening the agreement between experiment and calculation at larger x. Since whatever mechanism is responsible for the discrepancy at large x may also affect the phase boundary, it is not convincing to determine the parameters U_2 and U_3 by matching the calculated and experimental positions of the phase boundary, and the possible error in the absolute values of x of as much as 0.1 would make such a determination even less meaningful.

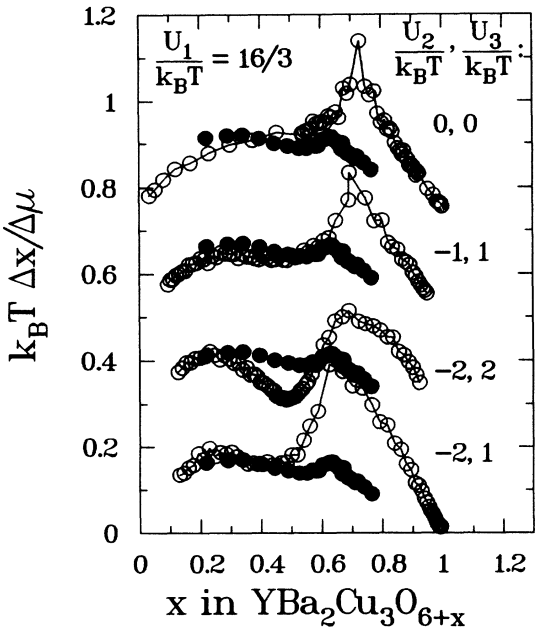

FIG. 9. Comparison of calculated $(\partial x/\partial \mu)_T$ (open circles) with the measured values from Fig. 4 (closed circles). The four series of points have been offset for clarity. Values of nearest-neighbor interaction U_1, next-nearest-neighbor interaction U_2 through Cu, and next-nearest-neighbor interaction U_3 not through Cu, are given in units of $k_B T$.

C. Behavior at low temperatures

From the comparison in Fig. 9, we can say only that U_2 and U_3 are probably less than or of order of $k_B T_0$ at $T_0 = 923$ K (about 0.06 eV). Values of $k_B T_0$, however, are large enough to allow the ordered phase at $x = 0.5$ to form between T_0 and room temperature. From MC calculations we estimate that this ordered state forms at $U_2 = -2.2 k_B T$ for $U_1 \gg k_B T$ and $U_2 = -U_3$. This agrees with the phase diagram of Ref. 29, where this phase appears when $U_2 > 2k_B T$. (Note that the interactions V in Ref. 29 are four times smaller than the interactions U used here, and that the phase diagram is plotted in units of $k_B T/V_1$.) If $U_2/k_B T_0 = -1$ at $T_0 = 923$ K, then the ordered state at $x = 0.5$ would appear near $T = T_0/2.2 = 420$ K. Thus values of U_2 and U_3 of about $k_B T_0$ can simultaneously be small enough not to affect the isotherm measured at 923 K and yet large enough to produce the ordered state at $x = 0.5$ somewhere between 923 K and room temperature.

Since the interaction U_2 is attractive, the transition between ordered states at low temperature will be first order, and so if these are the only interactions, then at zero temperature the phase diagram from $x = 0$ to $x = 1$ will consist of ordered states at $x = 0$, $x = 0.5$, and $x = 1$, and two-phase mixtures of these at intermediate x.[29] But in a real material the behavior at low temperatures will also be determined by the kinetics of phase separation caused by this attractive interaction. This attraction will cause the oxygens to cluster into chains even at low x. These chains will then interact, and one can imagine a variety of structures depending on how strong the interaction between chains is and how it varies with distance. There are analogies here to staging in graphite, where the intercalated atoms in the gap between a given pair of graphite layers attract one another, forming full gaps separated by empty ones. The full gaps then repel one another, leading to a series of phases with different separations of the full gaps.[12,30] In fact, for certain forms of the interaction between atoms in different gaps, it is in principle possible to obtain all possible sequences of full and empty layers, and the phase diagram would form a "devil's staircase" if the kinetics permitted.[31] Analogous structures of full and empty chains should be possible here, with further kinetic problems that result when chains growing along one crystallographic direction run into chains growing in the perpendicular direction.

Thus crystals at low x could be full of regions of different kinds of order. This could explain the broad transitions seen in Fig. 2. Both a distribution in the local oxygen concentration and a distribution in the local oxygen order could broaden the transitions. The point at

which the orthorhombic phase disappears in the lattice parameter in Fig. 1 probably depends on both kinetics and the strength of the interaction parameters, but the similarity of the lattice parameters for different ways of making the samples, and the similarity of the Meissner curves in Fig. 2 for samples prepared by removing or adding oxygen, suggests that this local structure is insensitive to the differences in these two ways of preparing samples. It might be, for example, that at temperatures two or three hundred degrees above room temperature, the kinetics of oxygen intercalation are governed by processes at the surface of the samples, rather than by oxygen diffusion within the bulk. Then oxygen would leave or enter the samples at a rate slow compared to the time to equilibrate the oxygen within the samples, so the composition of samples heated in argon would depend on the upper temperature reached, but the local order in these samples would be determined at lower temperatures as they cool.

VI. CONCLUSIONS

We have shown how a simple lattice-gas model with only nearest-neighbor interactions describes the thermodynamics of oxygen intercalation in the compound $YBa_2Cu_3O_{6+x}$, but with some discrepancy at high x. The discrepancies between the thermodynamic measurements and the lattice-gas models persist when second-neighbor interactions are included. Models that consider the interaction between ions and electrons, together with changes in the electronic structure with intercalation, might be more successful, but we caution that in such calculations it is essential to include the screening of the ionic charge by electrons, and the electronic structure of these materials is still being studied.

Our calculations show that the second-neighbor interactions between oxygen atoms can be large enough to produce ordered structures near $x=0.5$ at room temperature and yet small enough to have little effects on our thermodynamic measurements. The attractive interaction between O atoms separated by a Cu atom will lead to chains even at low x, and the details of the superconductivity and low-temperature structure will depend on how these chains are arranged, determined as much by kinetics as by thermodynamics.

ACKNOWLEDGMENT

We thank the Analytical Section of the Division of Chemistry at the National Research Council for chemical analysis.

[1]Y. Le Page, W. R. McKinnon, J. M. Tarascon, L. H. Greene, G. W. Hull, and D. M. Hwang, Phys. Rev. B **35**, 7245 (1987).

[2]J. E. Greedan, A. O'Reilly, and C. V. Stager, Phys. Rev. B **35**, 8770 (1987).

[3]K. Kamaras, C. D. Porter, M. G. Doss, S. L. Herr, D. B. Tanner, D. A. Bonn, J. E. Greedan, A. H. O'Reilly, C. V. Stager, and T. Timusk, Phys. Rev. Lett. **59**, 919 (1987).

[4]J. M. Tarascon, W. R. McKinnon, L. H. Greene, G. W. Hull, and E. M. Vogel, Phys. Rev. B **36**, 226 (1987).

[5]J. D. Jorgensen, M. A. Beno, D. G. Hinks, L. Solderholm, K. J. Volin, R. L. Hitterman, J. D. Grace, I. K. Schuller, C. U. Segre, K. Zhang, and M. S. Kleefisch, Phys. Rev. B **36**, 3608 (1987).

[6]H. Bakker, D. O. Welch, and O. W. Lazareth, Jr., Solid State Commun. **64**, 237 (1987).

[7]J. M. Sanchez, F. Mejia-Lira, and J. L. Moran-Lopez, Phys. Rev. B **37**, 3678 (1988).

[8]J. M. Tarascon, W. R. McKinnon, L. H. Greene, G. W. Hull, B. G. Bagley, E. M. Vogel, and Y. Le Page, in *Extended Abstracts of the Symposium on High Temperature Superconductors* (Materials Research Society, Pittsburgh, 1987), Vol. EA-11, p. 65.

[9]R. J. Cava, B. Batlogg, C. H. Chen, E. A. Rietman, S. M. Zahurak, and D. Werder, Nature **329**, 423 (1987).

[10]G. Van Tendeloo, H. W. Zandbergen, and S. Amelinckx, Solid State Commun. **63**, 603 (1987).

[11]L. T. Wille and D. de Fontaine, Phys. Rev. B **37**, 2227 (1988).

[12]S. A. Safran, Phys. Rev. Lett. **44**, 937 (1980).

[13]J. J. Murray, M. L. Post, and J. B. Taylor, J. Less Common Met. **80**, 201 (1981).

[14]Z. Z. Wang, J. Clayhold, N. P. Ong, J. M. Tarascon, L. H. Greene, W. R. McKinnon, and G. W. Hull, Phys. Rev. B **36**, 7222 (1987).

[15]P. K. Gallagher, H. J. O'Bryan, S. A. Sunshine, and D. W. Murphy, Mater. Res. Bull. **22**, 995 (1987).

[16]G. Xiao, F. H. Streitz, A. Gavrin, Y. W. Du, and C. L. Chien, Phys. Rev. B **35**, 8782 (1987).

[17]J. Hilsenrath, C. W. Beckett, W. S. Benedict, T. Fano, H. J. Hoge, J. F. Mass, R. L. Nuttall, Y. S. Touloukian, and H. W. Wooley, *Tables of Thermodynamic and Transport Properties* (Pergamon, New York, 1960), p. 369.

[18]J. R. Dahn and W. R. McKinnon, J. Phys. C **17**, 4231 (1984).

[19]A. J. Berlinsky, W. G. Unruh, W. R. McKinnon, and R. R. Haering, Solid State Commun. **31**, 135 (1979).

[20]W. R. McKinnon, Solid State Commun. **40**, 343 (1981).

[21]P. K. Gallager, Adv. Ceram. Mater. **2**, 632 (1987).

[22]K. Binder and D. P. Landau, Phys. Rev. B **21**, 1941 (1980).

[23]T. Muto and Y. Takagi, in *Solid State Physics,* edited by F. Seitz and D. Turnbull (Academic, New York, 1955), Vol. 1, p. 194.

[24]D. P. Landau, Phys. Rev. B **13**, 2997 (1976).

[25]R. KiKuchi, J. Chem. Phys. **60**, 1071 (1974).

[26]W. R. McKinnon and L. S. Selwyn, Phys. Rev. B **35**, 7275 (1987).

[27]J.Friedel, Adv. Phys. **3**, 446 (1954).

[28]R. M. Fleming, L. F. Schneemeyer, P. K. Gallagher, B. Batlogg, L. W. Rupp, and J. V. Waszczak, Phys. Rev. B **37**, 7920 (1988).

[29]L. T. Wille, A. Berera, and D. de Fontaine, Phys. Rev. Lett. **60**, 1065 (1988).

[30]J. R. Dahn, D. C. Dahn, and R. R. Haering, Solid State Commun. **42**, 179 (1982).

[31]P. Bak and R. Bruinsma, Phys. Rev. Lett. **49**, 249 (1982).